

# New Ratios for the Detection and Classification of CJD in Multisequence MRI of the Brain

Marius George Linguraru<sup>1,2</sup>, Nicholas Ayache<sup>1</sup>, Miguel Ángel González Ballester<sup>1,3</sup>, Eric Bardin<sup>4</sup>, Damien Galanaud<sup>3,6</sup>, Stéphane Haïk<sup>7,8,9</sup>, Baptiste Fauchoux<sup>7,8</sup>, Patrick Cozzone<sup>6</sup>, Didier Dormont<sup>4,5</sup>, and Jean-Philippe Brandel<sup>7,9</sup>

<sup>1</sup> EPIDAURE Research Group – INRIA Sophia Antipolis, France

<sup>2</sup> Division of Engineering and Applied Sciences, Harvard University, Cambridge MA, USA

<sup>3</sup> MEM-ISTB, University of Bern, Bern, Switzerland

<sup>4</sup> CNRS UPR640-LENA, Paris, France

<sup>5</sup> Department of Neuroradiology, La Pitié-Salpêtrière Hospital, Paris, France

<sup>6</sup> CRMBM UMR CNRS 6612, Faculty of Medicine, Marseille, France

<sup>7</sup> INSERM U360, La Pitié-Salpêtrière Hospital, Paris, France

<sup>8</sup> R. Escourolle Neuropathological Laboratory, La Pitié-Salpêtrière Hospital, Paris, France

<sup>9</sup> The National Reference Cell of CJD, La Pitié-Salpêtrière Hospital, Paris, France  
mglin@deas.harvard.edu

**Abstract.** We present a method for the analysis of deep grey brain nuclei for accurate detection of human spongiform encephalopathy in multisequence MRI of the brain. We employ T1, T2 and FLAIR-T2 MR sequences for the detection of intensity deviations in the internal nuclei. The MR data are registered to a probabilistic atlas and normalised in intensity prior to the segmentation of hyperintensities using a foveal model. Anatomical data from a segmented atlas are employed to refine the registration and remove false positives. The results are robust over the patient data and in accordance to the clinical ground truth. Our method further allows the quantification of intensity distributions in basal ganglia. sCJD patient FLAIR images are classified with a more significant hypersignal in caudate nuclei (10/10) and putamen (6/10) than in thalami. Defining normalised MRI measures of the intensity relations between the internal grey nuclei of patients, we robustly differentiate sCJD and variant CJD (vCJD) patients, as an attempt towards the automatic detection and classification of human spongiform encephalopathies.

## 1 Introduction

The identification of diagnosis markers is a major challenge in the clinical care of patients with Creutzfeldt-Jakob Disease (CJD). This disease raises a number of questions to neuroradiological centres, due to the limited available knowledge that connects it to medical imaging. Some recent studies [1,5,13] found strong correspondences between the diagnosis of CJD and the detection of signal abnormality in the deep grey matter internal nuclei in Magnetic Resonance Imaging (MRI) of the brain. However, the observations describing the MRI ability to help in the diagnosis of CJD are in an early stage. Most of the studies are concerned with sCJD cases, which represent 80% of all forms of CJD. The first study cases describe

hypersignals in T2-weighted images (and FLAIR-T2) with higher incidence in the basal ganglia in a bilateral symmetric form [1,6].

A great concern has been the occurrence in the United Kingdom of vCJD in the 1990s, a form of human environmentally acquired CJD. In FLAIR and T2 sequences, abnormal high signals are observed in the thalamus, mainly in the posterior pulvinar nucleus. Unlike in sCJD cases, in vCJD cases abnormal intensities are higher in the pulvinar when compared to striatum [13].

MR related image processing is an important tool in non-invasive CJD diagnosis [5,6]. At present time, MRI is not included as a diagnosis criterion for sCJD, which would be certainly useful to include, as for vCJD [13].

Leemput [12] proposes a method for automated quantification of MR intensity changes in images of CJD patients. A mixture model of normal distributions combined with the expectation-maximisation algorithm (EM) is proposed. However, the method does not detect signal abnormalities in all the CJD cases, while showing significant amounts of false positives (FP) along the interface between grey matter (GM) and cerebrospinal fluid (CSF).

Colchester, Hojjat *et al.* [3,7] analyse the putamen intensity gradient to separate CJD from normals and propose several ratios, (posterior thalamus to caudate and most notably to frontal white matter) to seclude vCJD from the rest. They use T2-weighted and Proton Density MRI for average intensities (no hyperintensity analysis) and their segmentation is performed manually.

The image blurring due to motion artefacts in the set of images of patients suffering of dementia makes the use of statistical detection algorithms very difficult. They need good contrast between GM and white matter (WM) for stochastic analysis according to a general atlas context. The approach we propose is based on image normalisation and the use of a priori anatomical knowledge in the form of an accurately segmented and labelled image (e.g. the Zubal Phantom [12]) for precise segmentation and of a probabilistic atlas for intra- and inter-patient analysis. A feature detection technique based on a model of the Human Visual System (HVS) is employed for the depiction of hypersignals. We differentiate different types of human prion diseases (sCJD from vCJD) based on the lesions topographical distribution.

## 2 Pre-processing and Segmentation

The sequences used by our algorithm are: a T1-weighted acquisition for its higher contrast between GM and WM and higher image resolution; T2-weighted images for the good contrast between CSF and brain parenchyma; and a T2-weighted FLAIR sequence for the detection of CJD signs in the brain. We use a model of data normalisation and regularisation, which is required to put the images in the same general framework to reduce the number of parameters. A review of the different stages of our segmentation algorithm is shown in Figure 1.

Data registration to an atlas has become a common technique with the introduction of popular statistical algorithms for image processing. A well-known probabilistic atlas in the scientific community is the MNI Atlas from the Montreal Neurological Institute at McGill University [4] built using over 300 MRI scans of healthy individuals. We used a block matching-based affine transformation described in [10] to register the patient T1, T2 and FLAIR images to the MNI atlas.

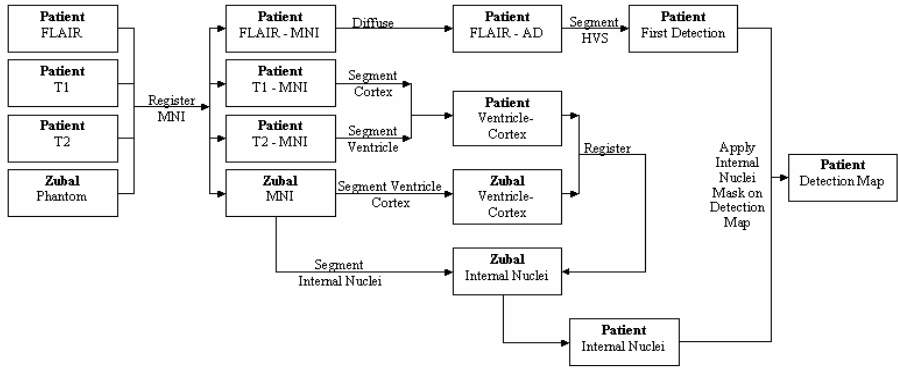


**Fig. 1.** Flowchart of the algorithm proposed for the detection of CJD-related abnormal hyperintensities in multisequence MRI of the brain

In addition to geometric variability, MR images may also exhibit intensity variations. Our method performs an affine equalisation using the joint histogram of two images [11]: a standard image (from our database) onto which we align the intensity distribution of the second image.

Our analysis is based on the abnormal MR intensities that can appear in the basal ganglia (including the thalamus) of CJD patients, which often show movement artefacts and therefore low contrast in images. The MNI atlas can provide a probabilistic segmentation of GM, which is not precise enough for our application. While avoiding direct non-rigid registration, the affine registration is approximate. We use instead a segmented anatomical atlas of the brain, the Zuhal Phantom [12].

The Zuhal atlas offers a precisely labelled segmentation of brain structures from the T1-weighted MR image of a single subject. First, the atlas must be aligned to our set of images; thus, we register the Zuhal Phantom to the MNI template, again using the block-matching algorithm [10]

Some important anatomical landmarks in the brain that are easier to identify are the ventricles and cortex external boundary. We segment them by morphological opening on patient T1 and T2 images. Ventricles will give a good approximation of the deformation field around the internal nuclei, whereas the cortex boundary will impose the global spatial constraints and stabilise the deformation field inside the brain. We are now in the possession of two binary maps of ventricles and brain boundaries for each patient: one from the Zuhal Phantom and the other from the patient. Non-rigid registration is used to align the two images and compute deformation fields, employing the iconic feature-based algorithm described in [2].

We create a mask with the pulvinar, “anterior thalamus” (the part of thalamus with small probability to show abnormal signals in CJD patients), putamen and head of the caudate - which will be referred as internal nuclei for the rest of this paper - from the Zuhal Phantom registered on MNI. Then we apply the above computed patient-specific deformation fields to the mask of internal nuclei of the Zuhal Phantom. The deformed mask is used to segment the internal nuclei on the patient image.

A foveal segmentation algorithm (HVS) [9] completes the detection of areas of CJD MR hypersignals in the brain. This is in essence an algorithm of adaptive

thresholding, which uses a mathematical model of human vision. A simplified model for the computation of the adaptive threshold  $C_{min}$  is shown in equation (1), where  $c_{mpc}$  is the minimal perceivable contrast,  $b$  is constant,  $\mu_N$  the mean value of the intensity of neighbourhood and  $\mu_A$  a mean weighted value of neighbourhood and background (entire image).

$$C_{min} = \frac{c_{mpc}}{\mu_N} \left( b + \sqrt{\frac{\mu_N^2}{\mu_A}} \right)^2 \tag{1}$$

$c_{mpc}$  must be computed as a function of the image gradient. In MR images of the brain, the intensity values of GM, WM and CSF can be regularised by intensity normalisation and  $c_{mpc}$  can be kept constant. Using an adaptive contrast measure both locally and globally, through the HVS foveal segmentation, our algorithm is less sensitive to artefacts, image quality and GM/WM contrast.

### 3 Intensity Quantitative Analysis

With the tools developed in this study, we can perform what seems to be the first computer-aided quantitative analysis between intensities in caudate nuclei or putamen, on one hand, and thalami (pulvinar nuclei and anterior thalami), on the other hand, for CJD patients. We will refer to it as Intensity Quantification Study (IQS).

We use the segmented putamen, caudate nuclei, pulvinar and anterior thalami on the patient images to compute the mean MR intensities in nuclei. We calculate the absolute values  $\Delta_1$  and  $\Delta_2$  as in equation (2) to represent the mean intensity differences for each patient and control, where  $\overline{Pul}$ ,  $\overline{Put}$ ,  $\overline{CN}$  and  $\overline{AT}$  represent the mean intensities respectively in the pulvinar, putamen, caudate nuclei and “anterior thalamus”.  $M$  represents the maximum value of all  $\Delta_1$  and  $\Delta_2$  over all controls.

$$\Delta_1 = \left| \overline{Put} - \overline{Pul} \right|, \Delta_2 = \left| \overline{CN} - \overline{Pul} \right|, M = \max_{controls}(\Delta_1, \Delta_2) \tag{2}$$

We define a first CJD prompting ratio ( $CP$ ) for the separation of CJD patients from healthy cases as in equation (3).  $CP$  reflects the value in each control that is closer to the patient data and therefore less discriminating, while in patients it highlights the most suspicious grey nuclei (as not all nuclei are affected in a patient and different types of CJD affect stronger different nuclei).

We further define a first CJD characterisation ratio ( $CC$ ) to differentiate between sCJD and vCJD based on the lesions topographical distribution, as in equation (3).  $\overline{HPul}$  and  $\overline{HCN}$  represent the mean hyperintense (abnormal) values (lesion specific) in the pulvinar and caudate nuclei.

$$CP = \max_{case}(\overline{Pul} / \overline{AT}, \overline{Put} / \overline{AT}, \overline{CN} / \overline{AT}), CC = \overline{HCN} / \overline{HPul} \tag{3}$$

### 4 Results

The database comprises a total number of 23 MR image sets acquired in two major neuroradiological centres of France: 10 sCJD cases (5 definite and 5 probable cases);

5 vCJD cases (2 definite and 3 probable cases with detection of PrPres in tonsil biopsy); and 8 healthy controls of similar ages to the patients. The images collected in Paris were acquired using a 1.5 Tesla GE Signa scanner: T1 (TE=20, TR=500), T2 (TE=92, TR=3000) and FLAIR-T2 (TE=148.5, TR=10002, TI=2200). The CJD data collected in Marseille were acquired using a 1.5 Tesla Siemens Magnetom Vision scanner: T1 (TE=15, TR=644), T2 (TE=22, TR=4000) and FLAIR (TE=110, TR=8000, TI=2200). Through intensity normalisation and the use of normalised ratios we can treat all data together for hypersignal segmentation.

Two radiological experts annotated all patient images. Figure 2 shows detection results on two patients with post-mortem neuropathologically confirmed CJD. The main radiological characteristic of the ten sCJD patients is the presence of higher intensities in the caudate nuclei and putamen. Strong thalamic abnormal intensity distributions are present in all vCJD cases, especially in the pulvinar. No false positive (FP) in are detected the control images.

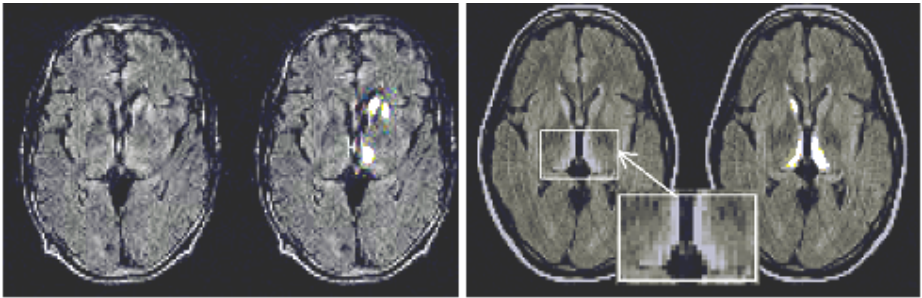


**Fig. 2.** Results on patient data – on the left an sCJD case with asymmetric lesions; on the right a vCJD case. We present a cross-section of each contrast-enhanced FLAIR MR data with abnormal hyperintensities in the internal nuclei; next to it we have the CJD detection map.

#### 4.1 CJD Prompting

For the intensity quantification (IQS), we prefer using FLAIR images before intensity normalisation (which was used for the hypersignal segmentation) for the most accurate estimation of mean values in the segmented internal nuclei. This naturally leads to different intensity values for the Paris ( $M=9.48$ ) and Marseille ( $M=25.63$ ) databases, as a result of using different MR scanners and acquisition protocols. The results are consistent over the sCJD patients and conform to the clinical observations, where cases can be differentiated from controls judging by the  $\Delta_1$  and  $\Delta_2$  values higher than  $M$ . There is no significant difference between mean intensities in putamen or caudate nuclei versus pulvinar for our control data.

We further compute the  $CP$  normalised measure for the entire database. We select the values in patient data that are greater than the highest value of all ratios over the control data (which is 1.155). All patient data provide at least one suspicious value higher than 1.155. All 10 sCJD cases show significant values in the caudate ratio, while 8/10 in the putamen ratio too. Four out of five vCJD cases present significant values in the pulvinar ratio, while 3/5 in the putamen and caudate nuclei, when mean intensities (not hyperintensities) over the entire nucleus are computed.

We box plot the value of  $CP$  into two groups: 1 - CJD cases (sporadic and variant together) and 2 - controls, as shown in Figure 3. For each group of data (CJD patients or controls), the plot shows the group median value (the bold central line), the minimum and maximum values (at the end of the dotted lines), the lower and upper quartiles (which enclose the box around the median), and the outliers (in circles). Performing a Welch Two Sample t-test between the two groups we get a value of  $p = 6.729e^{-6}$ , which gives an excellent separation between patients and controls with ratio mean values of 1.266 for CJD patients and 1.092 for controls.

## 4.2 CJD Characterisation

It is important to compute mean intensities over the entire nucleus (i.e. pulvinar, putamen or caudate) to be able to distinguish patients from controls (who have no hyperintensities in the deep grey nuclei). The addressed internal nuclei do not show hyperintensities for all patients; the caudate appears to be the only nucleus constantly affected. Furthermore, only parts of a nucleus may show hyperintensities and therefore the mean value computed over the entire nucleus does not always reflect the degree of abnormality in the respective patient nucleus. Therefore the need to concentrate on the hyperintense areas, rather than the entire nucleus. The abnormal intensities we will refer to are the hyperintensities found by our detection algorithm based on a foveal model (HVS).

We compute the  $CC$  ratio for each patient. All 10 sCJD cases have  $CC$  ratios greater than 1, while all 5 vCJD cases have  $CC$  ratios lower than 1. These results prove in a quantitative form that vCJD patients present higher abnormal intensities in the pulvinar than putamen or caudate nuclei, whereas sCJD patients show stronger hyperintensities in the caudate nuclei or putamen than pulvinar.

The box plot of the two patient subgroups is presented Figure 3. The two distributions are clearly different, as shown by the result of the Welch Two Sample t-test with a  $p$  value of  $5.865e^{-6}$ . The ratio mean values of the two classes are 1.190 for the sCJD and 0.967 for the vCJD.

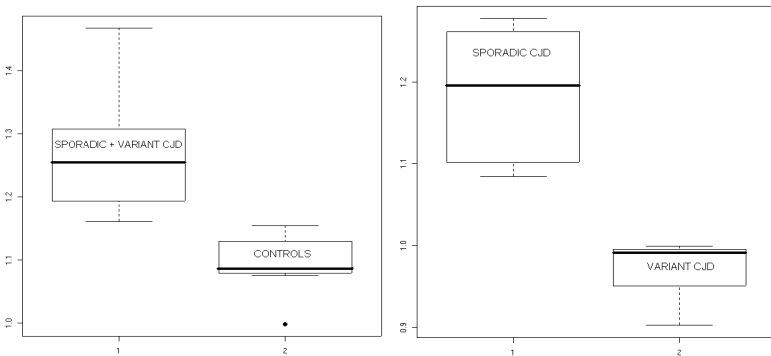


**Fig. 3.** Prompting and differentiating CJD: on the left the boxplot separating CJD patients (sCJD and vCJD together) from controls using the  $CP$  ratio shown on the vertical axis; on the right the boxplot separating sCJD patients from vCJD cases using the  $CC$  ratio shown on the vertical axis

The IQS separates on a first instance the CJD patients from healthy controls using the newly-defined *CP* ratio. Once the CJD cases isolated, we use the *CC* ratio to discriminate vCJD cases from sCJD. The IQS allows differentiating without ambiguity three distinctive classes: healthy controls, sCJD patients and vCJD patients. With a combination of HVS and IQS, we are able to prompt 15/15 prion disease cases with no FP amongst the controls and distinguish between sCJD and vCJD cases.

## 5 Discussion and Conclusion

We present a first attempt for quantitative numerical analysis of MR intensities of pulvinar versus putamen and caudate nuclei in FLAIR-T2 images of CJD patients. They accurately quantify the clinical remarks related to the possible classification of different types of human spongiform encephalopathies.

We define two new MRI-based ratios to prompt and differentiate CJD forms. All patients show abnormal intensities in the deep grey nuclei, which are correctly detected by our algorithm. All ten sCJD patients have higher mean intensities in the caudate nuclei and generally putamen. vCJD cases show more significant hyperintensities in the pulvinar than in the other deep grey nuclei, which makes them separable from the sCJD cases. All our experimental results are in complete accordance with the neurological findings in clinical practice and with the brain lesions profile described in each form of the disease.

In order to decrease the number of FP prompted by our detection algorithm, we refined the registration of the segmented data (the Zubal Phantom) on the patient specific data. We use intensity normalisation for the automated segmentation of hyperintensities, but the quantitative analysis is performed on the original values.

Quantifying the intensities in thalami, caudate nuclei and putamen, we show that there are always higher mean intensities in the caudate nuclei (10/10) and sometimes putamen (6/10) than the pulvinar of sCJD patients. The caudate nucleus is also of high intensity in the vCJD cases. This conclusion highlights the caudate nuclei as area of interest for the diagnosis of CJD, in complete agreement with the neuropathological findings. The relevance of caudate nuclei is also underlined by the decreased quantified mean ADC values in sCJD patients versus normal data (Diffusion Tensor and Diffusion Weighted images were available for some patients and controls in our database, but the results are preliminary).

The algorithm allows the study of asymmetries in CJD MR hypersignals, which has been long questioned by neuropathologists. Using basal ganglia masks, we also note that hypersignals are inhomogeneous over the nuclei.

We differentiate without ambiguity all CJD cases (sporadic and variant) from healthy controls and further characterise the CJD patients into two subgroups of human spongiform encephalopathies, sporadic and variant. More validation will be performed in future work, when more patient data are available.

The reader can refer to a detailed version of the methodology in this paper in [8].

We presented a method for the detection of hypersignals in grey matter internal nuclei from multisequence MR images. The particular context of our application is that of human spongiform encephalopathies, prion protein diseases referred as Creutzfeldt-Jakob Diseases (CJD). The technique employs intensity and spatial normalisation, foveal segmentation for the detection of hyperintensities and a priori

anatomical information for refined registration and removal of false positives. We are able to prompt 15/15 prion disease cases with no FP amongst the controls. Our method further allows the quantification of intensity distributions in basal ganglia, as we introduce two MRI-based ratios that discriminate between patients and normals and differentiate between CJD forms. The caudate nuclei are highlighted as main areas of diagnosis of sCJD, in agreement with the histological data. In vCJD patients, we find more significant hyperintensities in the pulvinar than in the other internal nuclei, which confirms the visually-based radiological observations related to CJD.

Our method proves as reliable as the visual interpretation of radiologists for the detection of basal ganglia hypersignals. Moreover, it allows to automatically obtain quantitative data from MR patients with CJD, which could be used for the follow-up of patients and evaluation of the efficiency of therapeutic procedures. Our study demonstrates the value of MRI for a prospective non-invasive diagnosis of sCJD and the characterisation of prion diseases, as we clearly differentiate sporadic from variant CJD cases. This work was partially funded by the GIS-Prions project.

## References

- [1] J.P. Brandel: Clinical aspects of human spongiform encephalopathies, with the exception of iatrogenic forms. *Biomed Pharmacother*, 53:14-18, 1999.
- [2] P. Cachier, E. Bardinnet, D. Dormont, X. Pennec, and N. Ayache: Iconic feature-based nonrigid registration: The PASHA algorithm. *CVIU* 89(2-3):272-298, 2003.
- [3] A.C.F. Colchester, S.A. Hojjat, R.G. Will and D. Collie: Quantitative Validation of MR Intensity Abnormalities in Variant CJD. In: *J.Neurol.Neurosurg.Psychiatry* 73(2): 213, 2002
- [4] D.L. Collins *et al.*: Design and construction of a realistic digital brain phantom. *IEEE Transactions on Medical Imaging*, 17(3):463-468, 1998.
- [5] M. Finkenstaedt, A Szudra, I. Zerr, S. Poser, J. Hise, J. Stoebner, and T. Wener: MR imaging of Creutzfeldt-Jakob disease. *Radiology*, 3:793-798, 1991.
- [6] H.J Gertz, H. Henkes, and J. Cervos-Navarro: Creutzfeldt-Jakob disease: Correlation of MRI and neuropathologic findings. *Neurology*, 38(9):1481-1482, 1988.
- [7] A. Hojjat, D. Collie, and A.C.F. Colchester: The putamen intensity gradient in CJD diagnosis. In *MICCAI 2002*, Vol. 2488 of LNCS, Springer, (2002) 524-531.
- [8] M.G. Linguraru *et al.*: Automated Analysis of Basal Ganglia Intensity Distribution in Multisequence MRI of the Brain – Application to CJD. *Res.Report RR-5276*, INRIA, 2004.
- [9] M.G. Linguraru, M. Brady, and R. English: Detection of Microcalcifications using SMF. In Peitgen, H.O. (ed.): *Digital Mammography*, Springer (2002) 342-346
- [10] S. Ourselin, A. Roche, S. Prima, and N. Ayache: Block matching: A general framework to improve robustness of rigid registration of medical images. In A.M. DiGioia and S. Delp, editors, *MICCAI 2000*, volume 1935 of LNCS, Springer (2000) 557-566,.
- [11] D. Rey, G. Subsol, H. Delingette, and N. Ayache: Automatic detection and segmentation of evolving processes in 3D medical images: Application to multiple sclerosis. *Medical Image Analysis*, 6:163-179, 2002.
- [12] K. Van Leemput: Quantitative Analysis of Signal Abnormalities in MR Imaging for Multiple Sclerosis and Creutzfeldt-Jakob Disease. PhD thesis, Kath. Univ. Leuven, 2001.
- [13] M. Zeidler *et al.*: The pulvinar sign on magnetic resonance imaging in variant Creutzfeldt-Jakob disease. *The Lancet*, 355:1412-1418, 2000.
- [14] I.G. Zubal, C.R. Harrell, E.O. Smith, Z. Rattner, G. Gindi, and P.B. Hoffer: Computerized dimensional segmented human anatomy. *Medical Physics*, 21:299-302, 1994.